Journal of Environmental Management 129 (2013) 423–434

Contents lists available at ScienceDirect

Journal of Environmental Management

journal homepage: www.elsevier.com/locate/jenvman

Zinc and cadmium removal by biosorption on *Undaria pinnatifida* in batch and continuous processes

J. Plaza Cazón, M. Viera*, E. Donati, E. Guibal [1]

Centro de Investigación y Desarrollo en Fermentaciones Industriales, CINDEFI (CCT CONICET La Plata, UNLP), Facultad de Ciencias Exactas, 50 y 115, 1900 La Plata, Argentina

ARTICLE INFO

Article history:
Received 27 November 2012
Received in revised form
17 June 2013
Accepted 8 July 2013
Available online 30 August 2013

Keywords:
Water treatment
Biosorption
Undaria pinnatifida
Heavy metals
Fixed bed column

ABSTRACT

Zn(II) and Cd(II) removal by biosorption using *Undaria pinnatifida* was studied in batch and dynamic systems. The kinetic uptake follows a pseudo second order rate equation indicating that the rate limiting step is a chemical reaction. The equilibrium data are described by the Langmuir isotherm in mono-component solutions. In binary solutions, the Jain and Snowyink model shows that most of the active sites are exclusively accessible to cadmium ions without competition with the zinc ions. The dynamic studies show that the biosorbent has higher retention and affinity for Cd(II) than for Zn(II) in both mono- and bi-component systems. SEM-EDX analysis indicates that the active sites are heterogeneously distributed on the cell wall surface. FT-IR spectrometry characterization shows that carboxylic groups and chemical groups containing N and S contribute to Zn(II) and Cd(II) uptake by *U. pinnatifida*. According to these results calcium-treated *U. pinnatifida* is a suitable adsorbent for Zn(II) and Cd(II) pollutants.

1. Introduction

Heavy metals are persistent contaminants that cannot be destroyed or degraded in the environment (Montazer-Rahmatia et al., 2011), representing an important problem with serious ecological and human health consequences. Thus, their elimination from industrial wastewaters is becoming an important challenge for Industry in relation with increasingly drastic national and international regulations (Bulgariu and Bulgariu, 2011). Biosorption is a remediation process that relies on the passive uptake of metal ions by inactive biomass. Metal biosorption is associated to the existence at biosorbent surface of ligands like carboxyl, sulphonate, amine, and hydroxyl groups, which have different affinity and specificity for metal binding. Brown algae are among the most promising biosorbent due to the density of carboxylic groups present in alginate (the main component of their cell wall), and to their availability and abundance in seas and oceans. To evaluate their maximum capacity and affinity, biomaterials have been tested, in most cases in mono-component experiments, mainly because the experimental design is simple to manage (Mata et al., 2008). However, real industrial wastewaters are characterized by the presence of several metal ions. For this reason, it is necessary to study the simultaneous adsorption of several contaminants. The models used to describe metal sorption from mono-component solutions cannot be used in binary systems since, in general, the sorption of one metal is influenced by the presence of the second one. Different mathematical models taking into account the competition between the adsorbates have been proposed for binary systems (Kleinübing et al., 2011).

Actual applications of biosorption imply the use of continuous–flow processes. Continuous packed bed adsorption columns are the most suitable systems for the removal of heavy metals as they are simple to operate, attain a high yield and can be easily scaled up for testing at pilot- or industrial-scale. In comparison with batch studies there have been few dynamic biosorption studies (Zhang and Banks, 2006). Apart from the practical importance, these kinds of studies also help in identifying the rate-limiting mechanism through the shape of the breakthrough curves. Desorption studies are important to evaluate biosorbent recycling and metal recovery.

The present work focuses on the sorption of Zn(II) and Cd(II) by *Undaria pinnatifida* in mono and binary systems. The main goals of our study are: a) the characterization of the biosorbent through the determination of the acid–base properties, SEM (Scanning Electron Microscopy) and EDX (Energy Dispersive X-ray) microanalysis, FT-

* Corresponding author. Present address: Centro de Investigación en Tecnologías de Pinturas, (CIDEPINT (CCT CONICET La Plata, CICPBA), Av. 52 y 121, B1900AYB La Plata, Argentina. Tel./fax: +54 221 4833794.
E-mail addresses: marisa.rviera@gmail.com, mviera@biotec.org.ar (M. Viera).
[1] Present address: Ecole des Mines d'Alès, Centre des Matériaux des Mines d'Alés, C2MA/MPA/BCI, 6 avenue de Clavières, 30319 Alès cedex, France.

0301-4797/$ – see front matter © 2013 Elsevier Ltd. All rights reserved.
http://dx.doi.org/10.1016/j.jenvman.2013.07.011

Nomenclature

a	constant of the dose − response model
b, b_1, b_2	Langmuir affinity constant of species 1 or 2 (L mmol^{-1})
B	activity coefficient related to biosorption mean free energy (mol J^{-1})
C_{eq}	final concentration at equilibrium (mmol L^{-1})
C_0; C_f	initial and final solute concentrations in solution (mg L^{-1} or mM), respectively
C_t; C_0	concentrations of sorbent at time t and zero (mg L^{-1}), respectively
C_{eff}	is the outlet metal concentration (mg L^{-1})
C_{eq1}	final concentration at equilibrium of species 1 (mmol L^{-1})
D.R	desorbed rate (%)
F_A	Feed velocity of the fixed bed per unit section transversal area of the bed (g cm^{-2} s^{-1})
K	constant related to the total affinity for both heavy metals in binary system (mmol L^{-1})
K_a	constant defined as the product of the Langmuir constants ($q_m b$) (L g^{-1})
K_{dif}	intraparticle diffusion rate constant
K_f	constant related to the biosorption capacity (mmol g^{-1})
k_1	rate constant (1 min^{-1})
k_2	pseudo-second order rate constant (g (mg min^{-1}))
k_{Th}	Thomas rate constant (mL min^{-1} mg^{-1})
k_{YN}	Yoon-Nelson rate constant
L	total length of the fixed bed (cm)
LUB	length of unused bed (cm)
m	mass of biosorbent (g)
M	biosorbent mass per unit of volume of solution (g L^{-1})
M_w	molecular weight (g mol^{-1})
m_d, m_b	metal mass desorbed and metal mass adsorbed (mg), respectively
m_l	total heavy metal loaded in the biomass (mg)
m_{total}	total metal mass sent to the column (mg)
MTZ	mass transfer zone (cm)
n	empirical parameter related to the biosorption intensity
q	solute uptake (mg g^{-1} or mmol g^{-1})
Q	is the volumetric flow rate (mL h^{-1})
q_{column}	capacity at exhaustion determine by the area below the breakthrough curve (mg g^{-1})
q_{eq}; q_t	sorption capacity at equilibrium and at time t (mmol g^{-1}), respectively
q_m	maximum Langmuir uptake (mmol g^{-1})
q_{m1}	maximum adsorption capacity of species 1 in presence of species 2(mmol g^{-1})
q_{mtotal}	total maximum capacity (species 1 + species 2) in binary system (mmol g^{-1})
q_{total}	total adsorption capacity (species 1 + species 2) at equilibrium in binary system (mmol g^{-1})
q_1	adsorption capacity of species 1 in presence of species 2 (mmol g^{-1})
R	gas constant, 8.314 J K^{-1} mol^{-1}
S_s	biosorbent surface area (m^2)
t_b	breakthrough time (h)
t_e	exhaustion operating time (h)
T	temperature (K)
UFB	unused fraction bed
V	solution volume (L)
V_{eff}	volume of metal solution passed through into column (mL)
W_b, W_{sat}	adsorbate loading, (g g^{-1}) in the breakthrough time and in the equilibrium, respectively

Greek symbols

β	activity coefficient (mol J^{-1})
β_L	external mass transfer coefficient (m s^{-1})
ε	Polanyi potential
τ	time required to reach 50% of total adsorption (on the breakthrough curve)
μ_0	superficial flow velocity (mL h^{-1})

IR (Fourier Transform Infrared) Spectroscopy analysis before and after metal uptake; b) the determination of kinetics and equilibrium parameters in batch systems in mono and binary Zn(II) and Cd(II) solutions, and c) the study of dynamic biosorption and desorption of Zn(II) and Cd(II) in fixed bed columns in mono and binary solutions.

2. Materials and methods

2.1. Biological material: pretreatment

The brown algae *Undaria pinnatifida* is invasive specie that produces undesirable changes in the biodiversity of the Argentinean Coast. Algae biomass used in this work was collected on the coast of Bahía de Camarones and Golfo Nuevo (Patagonia Argentina). It was ground and sieved and the 10–16 mesh (i.e., 1.18–2 mm) particle size fraction was selected, washed several times with distilled water and dried at 50 °C. Biomass was treated with 0.2 M $CaCl_2$ at pH 5.0 for 24 h. Then, it was repeatedly washed with distilled water and dried as mentioned before.

2.2. Physicochemical characterization of the biosorbent

Dry biological material (2.00 g) was weighed and placed in porcelain evaporating dishes and burned during 24 h at 405 °C. The percentage of organic matter was calculated by subtracting the ash weight to algae dry weight. The alginate extraction procedure was based on Arvizu-Higuera et al. (1995), with several modifications described in Plaza Cazón et al. (2012).The ion-exchange capacity of the biomass to bind cations, i.e. the number of negatively charged sites per unit of biomass mass, could be quantitatively expressed in a measured property known as Cation Exchange Capacity (CEC). The CEC was measured by cation displacement as described by Hawari and Mulligan (2006) and Plaza Cazón et al. (2012). The BET Surface Area was determined on approximately 1.00 g of biomass using krypton gas and a Coulter SA 3100 equipment (Beckman Coulter, USA). The analysis was performed in triplicates (Plaza et al., 2011).

Calcium treated biomass (2.00 g) was mixed for 1 h under agitation (160 rpm) with 100 mL of 0.10 M HCl. Then it was filtered, washed three times with distilled water and dried at 50 °C for 24 h. The amount of calcium released from the biomass was measured by atomic absorption spectrometry. The protonated biomass (0.10 g) was dispersed in flasks containing 100 mL of 1.0 mM NaCl solution. Titration was carried out by successive additions of standardized NaOH to the suspension that was maintained in agitation under nitrogen atmosphere. After each addition, the system was allowed to equilibrate and the pH was recorded using a pH-meter (ORION 3 STAR pH Benchtop-Thermo Electron Corporation, Singapore). Potentiometric titrations were performed in triplicate.

2.3. Batch sorption studies

Individual solutions of Zn(II) and Cd(II) at a concentration of 50 mg L^{-1} were prepared by dilution of the stock solution (1000 mg Zn(II) L^{-1} and 1000 mg Cd(II) L^{-1}, respectively) 100 mL-flasks volume capacity. The stock solutions of Zn(II) and Cd(II) were prepared by dissolving $ZnSO_4 \cdot 7H_2O$ (Biopack, Argentina) and $3CdSO_4\ 8H_2O$ (Baker-Analyzed, USA), respectively in distilled water. The individual solution pHs were adjusted at different initial values (i.e., 3.0, 4.0 and 5.0) by the addition of H_2SO_4. The concentration of treated biomass was set to 0.2% w/v for kinetic studies. Flasks were maintained under agitation at 160 rpm and placed in a controlled-temperature room at 20 ± 1 °C. Samples were collected at different intervals during 24 h and filtrated through 0.45 μm membrane. Metal concentrations in the liquid phase were determined using an atomic absorption spectrophotometer Shimadzu AA6650 (Shimadzu Corporation Kyoto, Japan). The pH was measured using a pH-meter (ORION 3 STAR pH Benchtop- Thermo Electron Corporation).

Zinc and cadmium sorption isotherms were obtained by mixing 0.1 g biomass with 100 mL of the metal-containing solution (with initial concentration between 10 and 400 mg L^{-1}; i.e., 0.15–6.11 mM Zn(II) and 0.089–3.57 mM Cd(II)). pH values of Zn(II) and Cd(II) solutions were set to pH 4.0 and pH 3.0, respectively. All flasks were kept in agitation at 160 rpm and 20 °C for 2 h. The optimum pH and the contact time were selected on the basis of kinetic studies. Samples were collected, filtrated through 0.45 μm membrane and the metal concentrations in the liquid phase analyzed by Inductively Couple Plasma Atomic Emission Spectroscopy (ICP-AES) using a JY 2000 spectrometer (Jobin-Yvon, Longjumeau,France).

To study the adsorption capacities for Zn(II) and Cd(II) when both metal ions were simultaneously present, mixed solutions were prepared at pH 4.0. The initial concentrations of each metal were equal and varied from 0.05 to 2.5 mM. All the other experimental conditions were the same as in mono-component batch adsorption.

2.4. Adsorption and desorption of heavy metals in fixed bed columns

A glass tube with 2.5 cm inner diameter and 15 cm length was used. The void volume of the packed column was 65 mL. 5.210 g of biomass was packed in the column, yielding an approximate bed length of 6 cm. At the top and the base of the column, a layer of glass wool was placed to prevent clogging of the hose. Previous to the beginning of the operation, distilled water was pumped to avoid a sudden initial increase in the metal initial concentration due to rapid absorption of water by the dried seaweed. The metal solutions were fed upward through the column at 100 mL h^{-1} using a peristaltic pump (Watson Marlow 101 U/R). This procedure facilitates the homogeneous contact between the solution and the biosorbent, and avoids the formation of preferential channels. Effluent was collected from the top of the column to analyze metal, calcium and sodium concentrations in the liquid phase using an atomic absorption spectrophotometer Shimadzu AA6650 (Shimadzu Corporation Kyoto, Japan) and pH measurement using a pH-meter (ORION 3 STAR pH Benchtop- Thermo Electron Corporation, Singapore). At the end of the experiment, 500 mL of distilled water was pumped into the column to remove any residual metal ions. Then, the biosorbent was taken out from the column and washed with distilled water, dried in oven at 50 °C for 24 h. The loaded-biomass was stored for the desorption process.

Desorption studies were also carried out in dynamic systems. Loaded-biomass (4.43 ± 0.10 g) from mono- and bi-component dynamic adsorption experiments was packed into the column. The eluent, 0.1M HNO_3, was fed upward at the flow rate 100 mL h^{-1}. The effluent was collected from the top of the column at different times and metal concentration in the liquid phase was determined using an atomic absorption spectrophotometer Shimadzu AA6650 (Shimadzu Corporation Kyoto, Japan). Effluent pH was also recorded.

2.5. SEM-EDX, FT-IR analysis

After metal sorption and desorption experiments, a sample of biosorbent was recovered, washed three times with distilled water and dried at 50 °C for 24 h and used for SEM-EDX and FT-IR analysis.

Samples were examined using SEM (Quanta FEG) equipped with EDX (OXFORD Inca 350). FT-IR analysis was performed using Nicolet 740 FT IR spectrometer (Perkin Elmer). Infrared spectra were recorded at a resolution of 2 cm^{-1} using 32 scans and the OMNIC software version 4.1 for numerical treatment of spectra. Analysis was performed on KBr discs: dry biomass carefully grounded was mixed with KBr (final concentration of sorbent in the powder close to 0.1% in weight), dried under vacuum before being conditioned in the form of thin discs (about 1.5 mm) under mechanic press (Svecova et al., 2006).

2.6. Analytical methods

The amount of metal adsorbed per mass unit of biosorbent (q) was calculated by the mass balance equation:

$$q = \frac{V\left(C_0 - C_f\right)}{m} \tag{1}$$

The results from kinetic and equilibrium experiments in batch system in mono and bi-component solutions were analyzed using different models, which can be found in Table SD1.

The amount of metal ion adsorbed into the biosorbent in column experiments was calculated on the basis of experimental breakthrough curves using the following equation (Wilson et al., 2012):

$$q_{\text{column}} = \int_{t=0}^{t=t_e} \left(\frac{C_0 - C_{\text{eff}}}{m}\right) \mathrm{d}t \tag{2}$$

The total heavy metal amount fed into the column, m_{total} (mg) could be calculated by the following equation:

$$m_{\text{total}} = \frac{C_0 Qte}{1000} \tag{3}$$

Also, the breakthrough curve allowed calculating others parameters, such as the mass transfer zone (MTZ) and the length unused bed (LUB) frequently calculated for evaluating the effective height of a sorption column. So, as the LUB becomes longer, efficiency of adsorption bed is decreased. MTZ and LUB can be calculated using the following equations (Lee et al., 2008):

$$F_A = \mu_0 C_0 M \tag{5a}$$

$$W_{\text{sat}} = \frac{F_A t_e}{m} \tag{5b}$$

$$W_b = \frac{F_A t_b}{m} \tag{5c}$$

$$\frac{W_b}{W_{\text{sat}}} 100\% = \text{UFB} \tag{5d}$$

$$\mathrm{MTZ} = L\left(\frac{t_e - t_b}{t_e}\right) \tag{4}$$

$$\mathrm{LUB} = \frac{\mathrm{UFBL}}{100} \tag{5e}$$

The results from continuous assays were fitted employing the equation models presented in Table SD 2.

The quantity of metal stripped out of the column in the desorption experiments was calculated by the equation (Zhang and Banks, 2006):

$$m_d = \sum C_i v_i \tag{6}$$

Where m_d is the metal stripped out of the column, C_i is the effluent metal concentration at the i fraction; v_i is the fraction i volume. The desorption ratio (D.R) was calculated from the amount of metal ions desorbed and the total metal loaded in the biomass using the following equation (Zhang and Banks, 2006):

$$\mathrm{D.R} = \frac{m_d}{m_l} 100 \tag{7}$$

3. Results and discussion

3.1. Physicochemical characterization of the biosorbent

The sorption properties of an adsorbent, like its capacity, can be improved or changed by several pre-treatments which can modify the surface characteristics/groups or contribute to exposing more metal binding sites (Oliveira et al., 2011). Physical pre-treatments may consist of heating/boiling, freezing/thawing, drying and freeze-drying. Chemical pre-treatments may proceed by washing the biomass with detergents, cross-linking with organic solvents and/or treatment with alkali or acid. Surface modification by calcium chloride, formaldehyde and glutaraldehyde treatments prevents the leaching of adsorptive components from biomass into the solution, increasing the stability of the biosorbent material, reducing the swelling of algal biomass (Boschi et al., 2011). In addition, the release of organic material from the biomass may contribute to complexation of the metal ions in solution, which, in turn, limits their availability for binding on the biosorbent (Matheickal and Qiming, 1999). The modification of the cell wall can significantly enhance metal binding capacity without affecting biosorption kinetics (Plaza et al., 2012).

The alginic acid may be present both in the cell wall matrix and in the mucilage or intercellular material and can constitute between 10 and 40% of the dry weight of the algae (Volesky, 2003). The yield of alginate found in this work for *U. pinnatifida* (Table 1) was in the same order of magnitude (around 30%) as other species of brown algae such as *Sargassum* sp., *Turbinaria* sp. and *Hormophysa* sp. (Rahelivao et al., 2013). The CEC was 69 meq (100 g)$^{-1}$ (Table 1) which was lower than that reported for anaerobic sludge biomass (94 meq (100 g)$^{-1}$) from UASB reactor cheese production used for heavy metal uptake (Hawari and Mulligan, 2006). *U. pinnatifida* specific surface area obtained by the BET method was 0.3 m^2 g^{-1}, this data would be compared with the specific surface area of *Fucus serratus* (0.22 m^2 g^{-1}), both values were low in relation with conventional porous materials (Ahmady-Asbchin et al., 2008).

Table 1
Physicochemical characteristics of *Undaria pinnatifida*.

Organic matter [%]	Alginate [%]	CEC [meq (100 g)$^{-1}$]	Specific area (BET) [m^2 g^{-1}]
88.7	30	69	0.3

The potentiometric titration of the protonated calcium-treated biomass is showed in Fig. 1A, while Fig. 1B shows the first derivative plot of the average titration curve. The first inflexion point and the last inflection point in Fig. 1B correspond to the strong acid groups and the total amount of acid groups, respectively (Oliveira et al., 2011). The total amount of acid groups was 0.46 mmol g^{-1} of which 0.07 mmol g^{-1} corresponded to the strong acid groups and the difference (0.39 mmol g^{-1}) to the weak acid groups. Strong acid groups have been identified as sulfonate groups while weak acid groups are mainly constituted by carboxylate groups from alginate, which represents more than 84% of the total acid groups (Oliveira et al., 2011).

During protonation of the calcium-treated biomass, 0.13 mmol g^{-1} of calcium ions bound to the biomass exchanged with protons. As calcium has two positive charges, 0.26 mmol g^{-1} of proton was needed to replace the calcium present on the cell wall, meaning that about 56% of the total acid groups were occupied by calcium as a consequence of the applied pretreatment.

3.2. Kinetic studies

The study of the variation of the metal uptake as function of time at different pH values is relevant from a practical point of view, because it allows choosing optimal conditions for the biosorption process such as equilibrium time and optimal pH for uptake but also it allows determining the limiting step that controls the binding kinetics.

Fig. 2 shows Zn(II) and Cd(II) adsorption kinetic on *U. pinnatifida*. The uptake proceeded in two steps: a fast uptake rate in the first 60 min, where more than 75% of metal adsorption occurred, followed by a slower uptake rate as equilibrium is approaching. The equilibrium was reached within 120 min for each metal.

The controlling step in the sorption process can be the diffusion of the adsorbate (which involves three steps: bulk, film and intraparticle diffusion) or the reaction rate. All the kinetic models presented in the Supplementary Data Section (Table SD1) were applied to the data presented in Fig. 1. Table 2 shows that the best fitting in the whole data range was found using the pseudo-second order rate equation (PSORE). In this model, the rate-limiting step is the chemical reaction or chemisorption, where metal removal from solution is due to purely physical–chemical interactions between biomass and metal ions (Lodeiro et al., 2006). According to Ho (2006), if heavy metal uptake is chemically controlled, the PSORE constants will be independent of particle diameter and flow rate and will depend on another variable like the pH or the temperature of the solution. The same conclusion was found in the case of the biosorption of Zn(II) and Cd(II) by calcium-treated *Macrocystis pyrifera* (Plaza et al., 2012).

3.3. Optimum pH

A number of studies have pointed out the effect of pH on biosorption efficiency (Montazer-Rahmatia et al., 2011; Gupta et al., 2001). However, the ANOVA applied for comparing the final uptake of each metal ions by *U. pinnatifida* for all tested pH values shows that there are no significant differences among them ($F_{\mathrm{calculated}} < F_{\mathrm{theoretical}}$, with $\alpha = 0.05$). Thus, the pH chosen for the equilibrium studies were pH 3 for Cd(II) solutions and pH 4 for Zn(II) solutions, in accordance with those used in the adsorption of same metals by another species of brown alga (*M. pyrifera*) (Plaza et al., 2012).

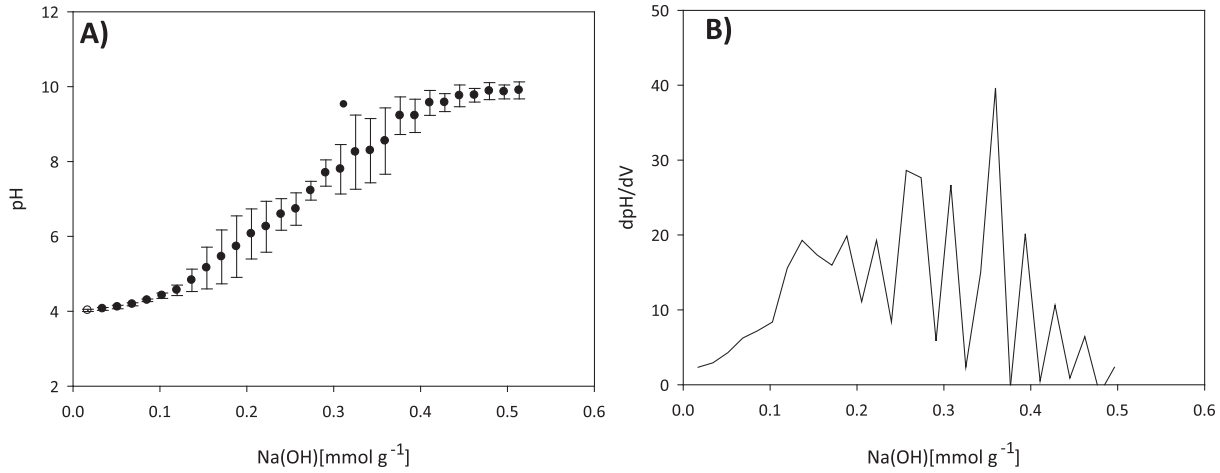

Fig. 1. A) Potentiometric titration curve of protonated calcium-treated *U. pinnatifida*. B) First derivative curve of average pH during the titration.

3.4. Adsorption isotherms in mono-component systems

The isotherms plots for each heavy metal were represented in Fig. 3. Metal adsorption increases with residual metal concentration for both Zn(II) and Cd(II) before stabilizing (saturation plateau) at high metal concentration. This shape is typical of the Langmuir equation. Table 3 reports the parameters of the Langmuir and Freundlich models (together with their correlation coefficients). Experimental data exhibited a good fitting with both models. In mono-component systems, the maximum adsorption capacity (q_m) for Zn(II) (1.53 mmol g^{-1}) was higher than for Cd(II) (1.08 mmol g^{-1}) while the affinity coefficient (b) presented the opposite behavior. The same results were found by others authors (Luna et al., 2010). They justified their results based on the differences in the hydrated ionic radii (Zn(II) = 6 Á and Cd(II) = 5 Á) (Luna et al., 2010). Other possible explanation is based on the occurrence of different metal-binding mechanisms (ion-exchange, complexation, coordination, and micro-precipitation) that depend on the chemical groups present on the cell wall of the biomaterial and also on the acid-base properties of the metal ions. According to the Hard and Soft Acid Base (HASB) principle, Cd(II) is a soft Lewis acid, while Zn(II) is a borderline acid so they show differences in their preference for the ligands: Zn(II) forms strong complex with electronegative elements (such as F and O) while Cd(II) forms strong bound with ligands such as S or P. The presence of chemical groups containing these elements was confirmed by FT-IR analysis (see Section 3.7).

The values of q_m for each heavy metal were compared with those reported in the literature (Table 4). *U. pinnatifida* exhibits a higher efficiency for Cd(II) recovery than other adsorbents as red mud (q_m = 0.95 mmol g^{-1}) (Ahmaruzzaman, 2011), agave bagasse modified with 1M HNO_3, HCl, NaOH (q_m = 0.067, q_m = 0.11, q_m = 0.11 mmol g^{-1}, respectively) (Velazquez-Jimenez et al., 2013), activated sludge (from wastewater bioethanol treatment) (q_m = 0.51 mmol g^{-1}) (Remenárová et al., 2012), *Fontinalis antipyretica* (moss) (q_m = 0.25 mmol g^{-1}) (Martins et al., 2004) and different algae biomass such as *Padina* sp. (q_m = 0.75 mmol g^{-1}), *Sargassum* sp. (q_m = 0.76 mmol g^{-1}), *Ulva* sp. (q_m = 0.58 mmol g^{-1}), *Gracilliaria* sp. (q_m = 0.30 mmol g^{-1}) (Sheng et al., 2004), *Fucus vesiculosus* (q_m = 0.96 mmol g^{-1}) (Mata et al., 2008), *Lessonia nigrescens* (q_m = 0.99 mmol g^{-1}; pH 6) (Boschi et al., 2011), *Sargassum filipendula* (q_m = 1.03 mmol g^{-1}) (Luna et al., 2010), *S. filipendula* (q_m = 0.63 mmol g^{-1}) (Fagundes-Klen et al., 2007), formaldehyde-treated *Cystoseira indica* (q_m = 0.17 mmol g^{-1}) (Montazer-Rahmatia et al., 2011), *Gymnogongrus torulosus* (q_m = 0.66 mmol g^{-1}) (Areco and dos Santos Afonso, 2010) and *M. pyrifera* (Ca-treated) (q_m = 0.87 mmol g^{-1}) (Plaza et al., 2012). Carbon activated carbon (oxidized ACF) (q_m = 1.3 mmol g^{-1}) (Kurinawan et al., 2006), flash ash (q_m = 1.76 mmol g^{-1}) (Ahmaruzzaman, 2011), and *L. trabeculata* (q_m = 1.47 mmol g^{-1}; pH

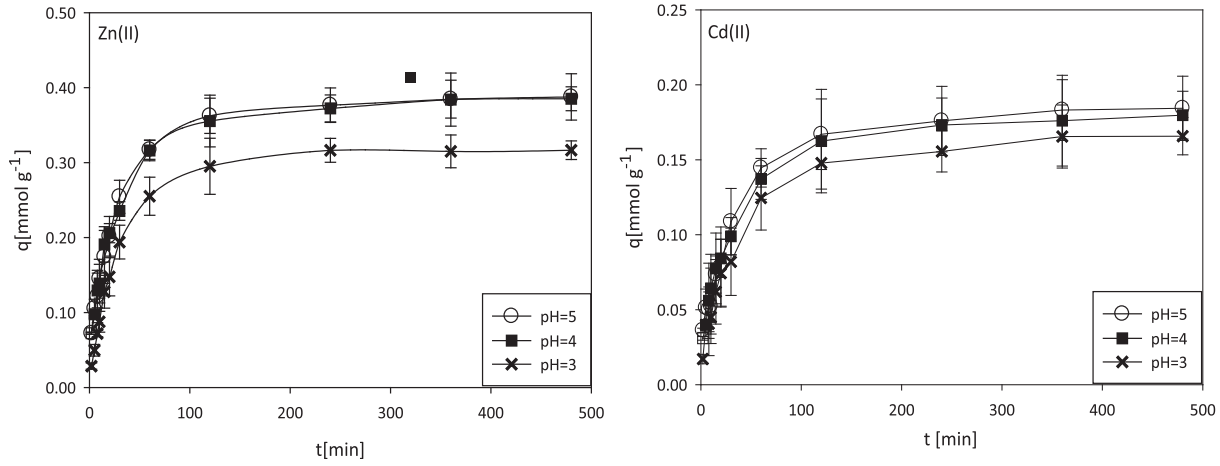

Fig. 2. Zn(II) and Cd(II) kinetics onto treated *U. pinnatifida*.

Table 2
Kinetic constants for Zn(II) and Cd(II) uptake onto treated *U. pinnatifida*.

Parameters	Zn(II)			Cd(II)		
	pH			pH		
	3	4	5	3	4	5
Pseudo first order rate equation						
q_{exp} (mmol g^{-1})	0.31	0.38	0.38	0.16	0.17	0.18
q (mmol g^{-1})	0.26	0.27	0.28	0.13	0.14	0.14
k_1 (min^{-1})	0.022	0.019	0.021	0.017	0.018	0.018
R^2	0.98	0.97	0.98	0.95	0.98	0.98
Pseudo second order rate equation						
q (mmol g^{-1})	0.34	0.39	0.40	0.17	0.18	0.19
k_2 (g mmol^{-1} min^{-1})	0.11	0.16	0.15	0.22	0.28	0.24
R^2	0.99	0.99	0.99	0.99	0.99	0.99
External mass transfer						
β_L (m s^{-1})	4.1×10^{-5}	8.0×10^{-5}	9.8×10^{-5}	7.9×10^{-5}	1.1×10^{-4}	1.5×10^{-4}
R^2	0.94	0.99	0.99	0.99	0.98	0.95
Intraparticle diffusion						
K_{id} (mmol g^{-1} min$^{-1/2}$)	0.029	0.0311	0.032	0.013	0.014	0.014
R^2	0.94	0.94	0.95	0.97	0.97	0.96

6) (Boschi et al., 2011) had higher Cd(II) adsorption capacity than *U. pinnatifida* biomass. However, *U. pinnatifida* exhibits a higher q_m for Zn(II) than all the adsorbents mentioned in Table 4.

The equilibrium data were also analyzed with the Dubinin–Radushkevich isotherm and the mean biosorption energy (E; kJ mol^{-1}) was estimated to characterize the nature of the process (physical versus chemical adsorption). If the E value is between 8 and 16 kJ mol^{-1}, the biosorption proceeds by chemical ion-exchange and if $E < 8$ kJ mol^{-1}, the biosorption process is of physical nature (Sari et al., 2007). E was calculated as 8.8 and 8.6 kJ mol^{-1} for the biosorption of Zn(II) and Cd(II) ions, respectively. These results show that the biosorption process of each metal ion onto *U. pinnatifida* proceeded through a chemical ion-exchange mechanism.

3.5. Adsorption equilibrium for Zn(II)–Cd(II) bi-component systems

The correct and most illustrative way of representing the biosorption equilibrium of a two-metal system is to construct 3-D sorption isotherm plots whereby the individual and total metal uptake are plotted as a function of the final equilibrium concentrations of both metals. For Zn(II)–Cd(II) bi-component system, these plots are presented in Fig. 4. A decrease in sorption of Zn(II) or Cd(II) occurred due to the presence of the competitor ion. Different models were used to analyse these data (see Supplementary Data Section). Table 5 reports the parameters found for the Competitive and Non- Competitive Langmuir models and for the Jain and Snowyink model. The last model assumes that a part of the adsorption occurs without competition. In the present case, the fraction of cadmium ions adsorbed without competition with zinc ions is defined by the difference ($q_{mCd} - q_{mZn}$), which accounted for 0.45 mmol g^{-1}, while the fraction of metal adsorbed under the control of competition effects is given by $q_{mZn} = 0.30$ mmol g^{-1}. This means that about 60% of the sites are exclusively accessible to cadmium ions (without competition) while the other 40% of the sites adsorbs cadmium and zinc, with competition. Competition between Zn(II) and Cd(II) ions for the binding sites was also found using other brown algae such as *M. pyrifera* (Plaza et al., 2012) and *S. filipendula* (Luna et al., 2010).

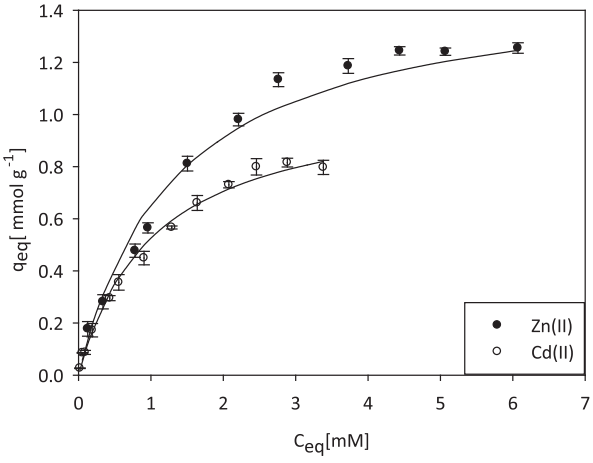

Fig. 3. Zn(II) and Cd(II) mono-component isotherm by calcium-treated *U. pinnatifida*.

The b values calculated with the Langmuir Competitive model indicated that the biosorbent had a preference for Zn(II) over Cd(II). This was not consistent with previous observation in mono-component systems. The maximum adsorption capacity for Cd(II) (q_{mCd}) in presence of Zn(II) was higher than the maximum adsorption capacity for Zn(II) (q_{mZn}) in presence of Cd(II) (Table 5). The q_{mZn} and q_{mCd} calculated by the modified Langmuir Competitive model gave lower values for each metal than those estimated by Langmuir model for mono-component system. However, the Langmuir Competitive (approximation) model gave the same q_{mZn} and q_{mCd} that those estimated by Langmuir model for mono-component system and also this model indicated that the biosorbent had significantly higher affinity for Cd(II) over Zn(II) consistent with previous observation in mono-component system. The total metal uptake value q_{Zn+Cd} determined by Langmuir No-competitive model was lower than the sum of individual q_{mZn} and q_{mCd} estimated by Langmuir model mono-component system

Table 3
Langmuir, Freundlich and Dubinin–Radushkevich parameters found for the adsorption of Zn(II) and Cd(II) by treated *U. pinnatifida*.

	Langmuir			Freundlich			D-R	
	q_m [mmol g^{-1}]	b [L mmol^{-1}]	R^2	K_f [mmol g^{-1}]	n	R^2	E [kJ mol^{-1}]	R^2
Zn(II)	1.53	0.75	0.98	0.54	1.72	0.98	8.83	0.99
Cd(II)	1.08	0.96	0.98	0.45	1.51	0.98	8.57	0.99

Table 4
The maximum adsorption capacity (q_m) of different adsorbents in mono-component batch systems.

Biosorbents	Znq_m [mmol g^{-1}]	Cdq_m [mmol g^{-1}]	References
Activated carbon	0.3(GAC type C)	1.3(oxidized ACF)	Kurniawan et al., 2006
Natural zeolite	0.19		Peric et al., 2004
Flash ash	0.099	1.76	Ahmaruzzaman, 2011
Red mud	0.19	0.95	Ahmaruzzaman, 2011
HN-AB (agave bagasse modified with 1M HNO3)	0.16	0.067	Velazquez-Jimenez et al., 2013
HC-AB (agave bagasse modified with 1M HCl)	0.18	0.11	Velazquez-Jimenez et al., 2013
Na-AB (agave bagasse modified with 1M NaOH)	0.31	0.11	Velazquez-Jimenez et al., 2013
Activated sludge (from wastewater bioethanol treatment plant)	0.54	0.51	Remenárová et al., 2012
Fontinalis antipyretica (moss)	0.22	0.25	Martins et al., 2004
Padina sp.	0.81	0.75	Sheng et al., 2004
Sargassum sp.	0.50	0.76	Sheng et al., 2004
Ulva sp.	0.54	0.58	Sheng et al., 2004
Gracillaria sp.	0.40	0.30	Sheng et al., 2004
Fucus vesiculosus		0.96	Mata et al., 2008
Lessonia nigrescens		0.99	Boschi et al., 2011
L. trabeculata		1.47 (pH 6)	Boschi et al., 2011
Sargassum filipendula	0.68		Boschi et al., 2011
S. filipendula		1.03	Luna et al., 2010
S. filipendula		0.63	Fagundes-Klen et al., 2007
Cystoseira indica (formaldehyde-treated)		0.17	Montazer-Rahmatia et al., 2011
Gymnogongrus torulosus	0.68	0.66	Areco and dos Santos Afonso, 2010
M. pyrifera (Ca-treated)	0.67	0.87	Plaza Cazón et al., 2012
U. pinnatifida (Ca-treated)	1.53	1.08	This study

(Tables 3 and 5), indicating that, in addition to the competition between metal ions, some of the Cd(II) and Zn(II) ions are taken up without mutual competition, and some active site may be specific to individual metals as it was confirmed with Jain and Snowyink model (Table 5). Fagundes–Klen et al. (2007) also investigated the simultaneous removal of Zn(II) and Cd(II) using *S. filipendula* treated with $CaCl_2$ (0.5M). The application of the modified Langmuir competitive model gave: $q = 0.54$ mmol g^{-1}, $b_{Cd} = 2.28$ L

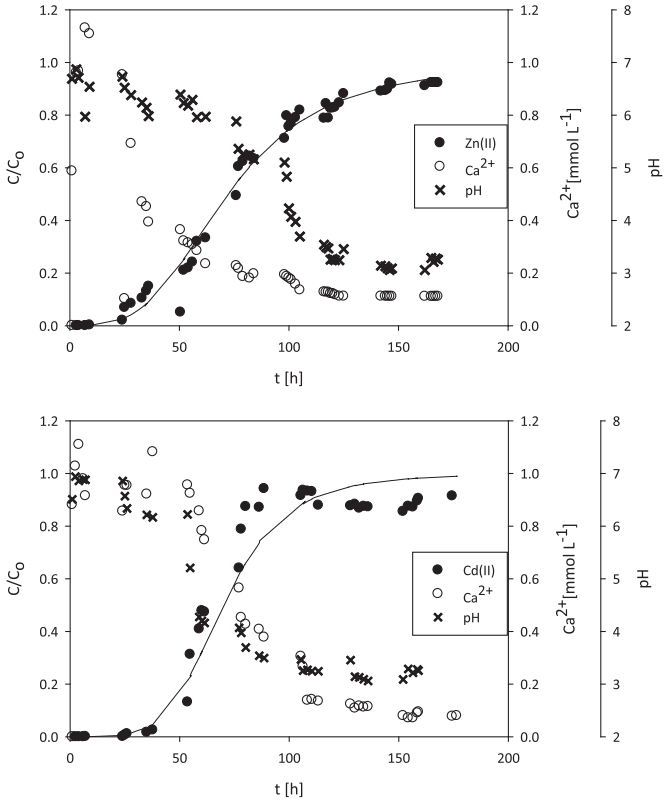

Fig. 4. 3-D plot of Zn(II) (●), Cd(II) (○)and total (Zn(II)+Cd(II)) (■) uptake in bi-component system by treated *U. pinnatifida*.

Table 5
Adsorption constants of Zn(II) and Cd(II) uptake on treated *U. pinnatifida* in bi-component solutions.

Models	Parameters
Theoretical	$q_{Zn+Cd} = 0.84$ mmol g^{-1}; $b_{Zn+Cd} = 2.8$ L mmol^{-1}; $R^2 = 0.98$
Langmuir competitive	$q_{mZn} = 0.35$ mmol g^{-1}; $b_{Zn} = 4.08$ L mmol^{-1}; $R^2 = 0.98$ $q_{mCd} = 0.88$ mmol g^{-1}; $b_{Cd} = 2.27$ L mmol^{-1}; $R^2 = 0.99$
Langmuir competitive (approximation)	$q_{mZn} = 1.53$ mmol g^{-1}; $b_{Zn} = 0.84$ L mmol^{-1}; $R^2 = 0.97$ $q_{mCd} = 1.08$ mmol g^{-1}; $b_{Cd} = 7.22$ L mmol^{-1}; $R^2 = 0.97$
Langmuir no-competitive	$q_{Zn+Cd} = 0.89$ mmol g^{-1}; $b_{Zn+Cd} = 7.75$ L mmol^{-1} $R^2 = 0.99$
Jain and Snowyink	$q_{mZn} = 0.30$ mmol g^{-1}; $q_{mCd} = 0.75$ mmol g^{-1} $b_{Zn} = 4.55$ L mmol^{-1}; $b_{Cd} = 4.58$ L mmol^{-1} $R^2 = 0.98$

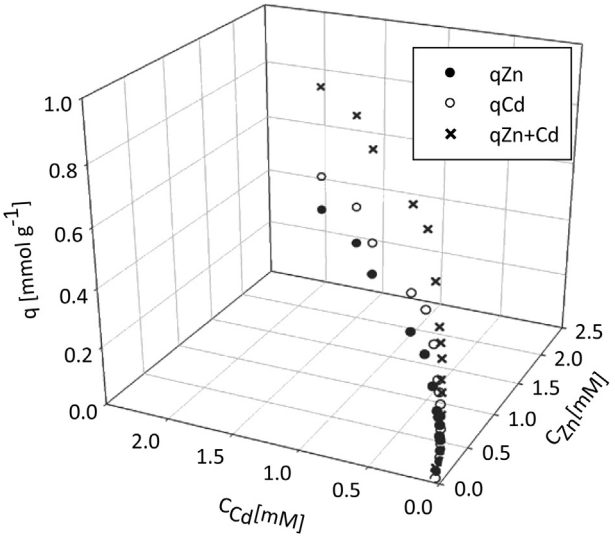

Fig. 5. Zn(II) and Cd(II) breakthrough curves in mono-component systems in fixed bed column filled with calcium-treated *U. pinnatifida*. Continuous lines represent the fitting with the Dose-Response model.

Table 6
Breakthrough curve, Thomas, Yoon-Nelson and Dose-Response models parameters for mono-component and bi-component systems using fixed bed columns with Ca-treated *U. pinnatifida*.

	Parameters	Mono-component		Bi-component	
		Zn(II)	Cd(II)	Zn (II)	Cd(II)
Breakthrough curve	t_b [h]	25	40	24	34
	t_e [h]	145	107	50	n.d
	V_b [mL]	2500	4000	288	408
	q [mg g^{-1}]	130.6	88.5	40.84	103.31
	LUB [cm]	1.02	2.22	2.88	0.19
	MTZ [cm]	4.96	3.75	3.12	4.72
	m_{total} [mg]	688.31	465.34	289.02	961.97
	% ads.	53.88	68.90	73.62	55.92
Thomas	K_{Th} [L mg^{-1} h^{-1}]	9.2×10^{-4}	1.6×10^{-3}	-2.6×10^{-3}	-7.8×10^{-4}
	q_0 [mg g^{-1}]	69.5	59.7	75.15	98.66
	R^2	0.99	0.98	0.97	0.96
	t_b [h]	9.35	30.7	1.47	1.02
	t_e [h]	50.3	115	59.7	95
	MTZ [cm]	4.88	4.39	5.85	5.93
Yoon Nelson	k_{YN} [h^{-1}]	0.043	0.0668	0.127	–
	τ [h]	76.02	71.19	37.10	–
	R^2	0.98	0.97	0.96	–
Dose-response	q_0 [mg g^{-1}]	65.8	58.4	39	91.8
	R^2	0.99	0.98	0.98	0.98

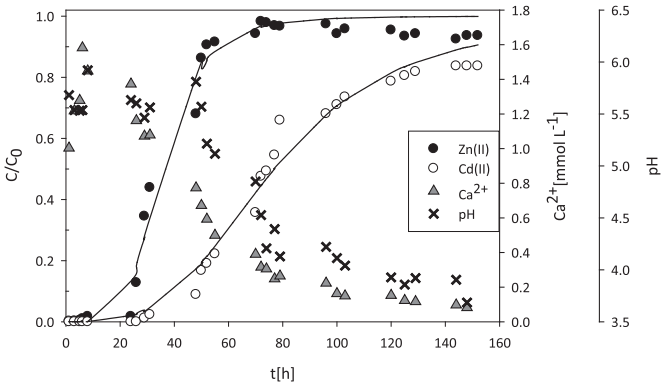

Fig. 6. Breakthrough curves for Zn(II) and Cd(II) adsorption in fixed bed column by *U. pinnatifida* in bi-component system. Continuous lines represent the fitting with the Dose-Response model.

mmol^{-1} and b_{Zn} = 4.78 L mmol^{-1}. In this case, the biosorbent presented a higher affinity coefficient for Zn(II) than for Cd(II), contrary to the present results. Consistently with this study, Luna et al. (2010) obtained the same order of affinity for zinc and cadmium using an untreated biomass of *S. filipendula* (q = 0.67 mmol g^{-1}, b_{Cd} = 19.34 L mmol^{-1} and b_{Zn} = 10.40 L mmol^{-1}) and Reménarová et al. (2012) found that dried activated sludge (DAS) in bi-component system Cd(II)–Zn(II) has significantly higher affinity for Cd(II) ions when Zn(II) are present in solution in equimolar ratio 1:1. Moreover, Plaza et al. (2012) found that *M. pyrifera* Ca-treated biomass had higher affinity coefficient for Cd(II) b_{Cd} = 7.66 L mmol^{-1} than for Zn(II) b_{Zn} = 4.55 L mmol^{-1} using the Langmuir Competitive model that was in agreement with the present results.

3.6. Dynamic studies

Before biosorption could be applied in the treatment of an industrial effluent it is necessary to investigate the process in a dynamic mode using fixed-bed columns. The efficiency of the

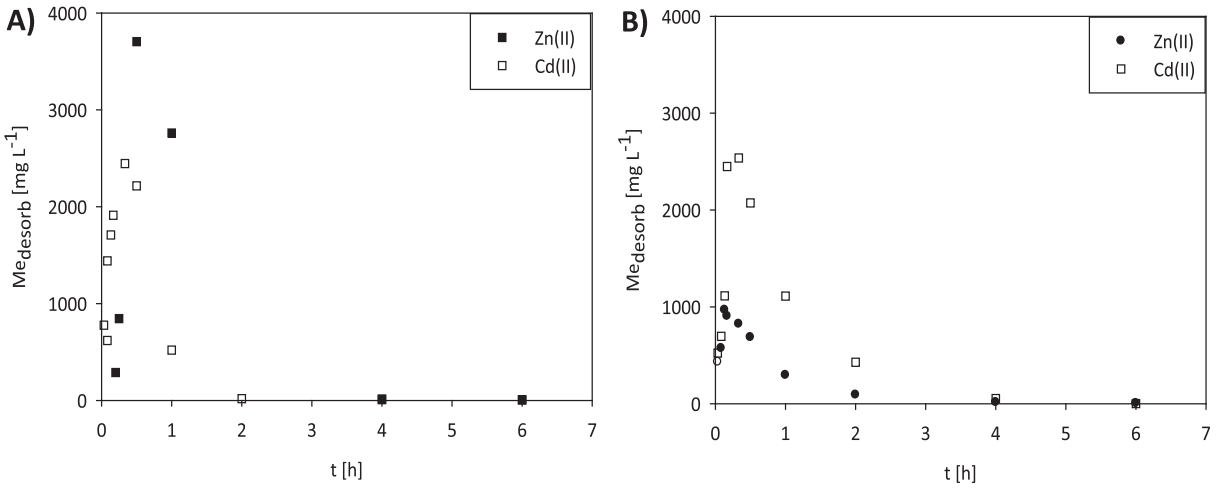

Fig. 7. Zn(II) and Cd(II) desorption column: A) from mono-component system; B) from Zn(II)–Cd(II) bi-component system.

columns is evaluated through the analysis of the breakthrough curves, where the ratio C_{eff}/C_o is plotted vs. the operating time or the effluent volume. The resulting breakthrough curves obtained with the fixed bed columns filled with *U. pinnatifida* and fed with Zn(II) or Cd(II) solutions are shown in Fig. 5. Table 6 presents the parameters obtained through the analysis of the breakthrough curves and the application of Thomas, Yoon-Nelson and Dose-Response models (see Supplementary Data section). The breakthrough time (t_b) is the time for complete metal recovery (full efficiency of the sorbent), and the saturation time (t_s) is the time

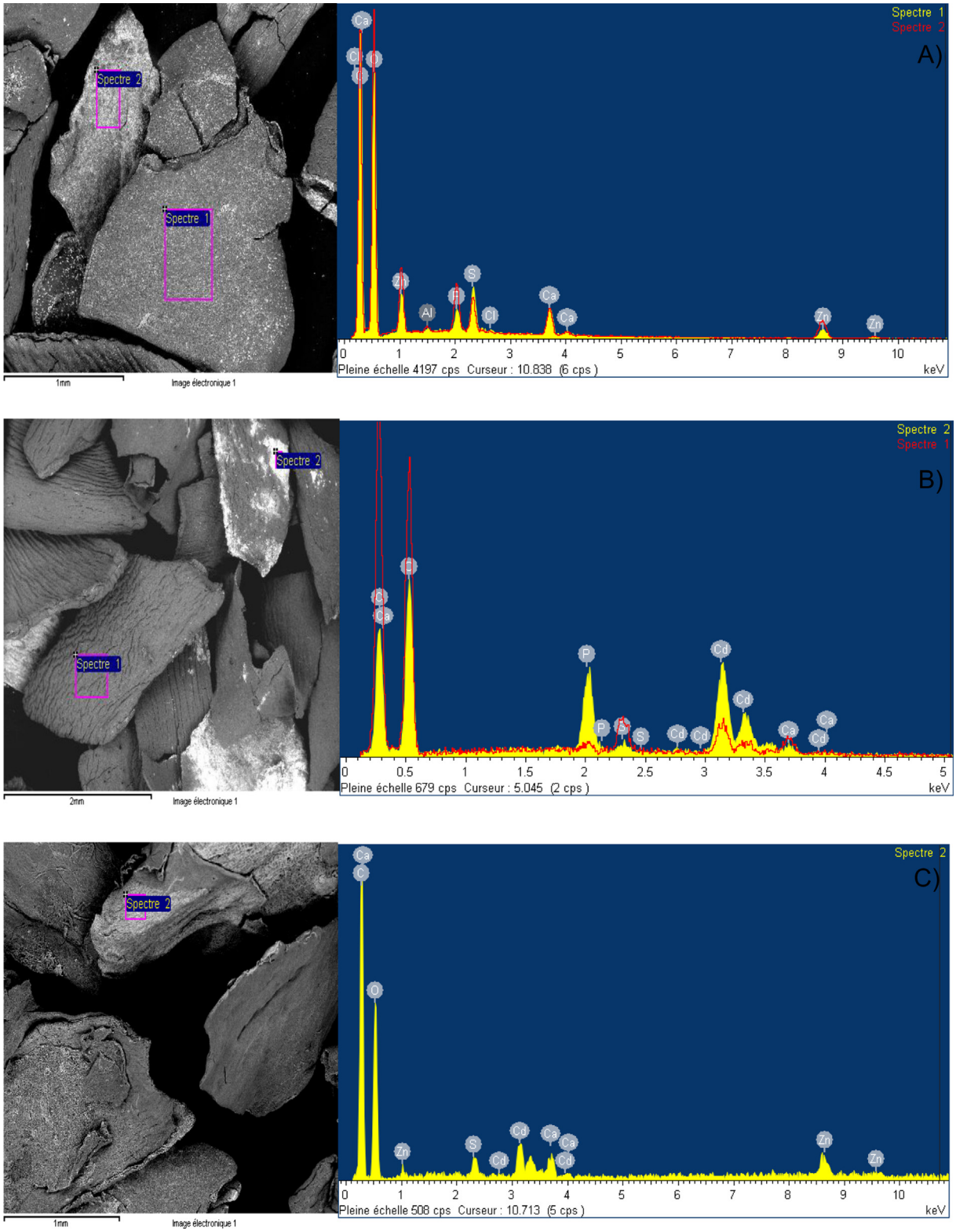

Fig. 8. SEM-EDX characterization of *U. pinnatifida* after Zn(II) and Cd(II) biosorption in batch system. A) Zn(II)-loaded biosorbent. The bar under the micrograph corresponds to 1 mm; B) Cd(II)-loaded biosorbent. The bar under the micrograph corresponds to 2 mm; C) Zn(II)+Cd(II)-loaded biosorbent. The bar under the micrograph corresponds to 1 mm.

corresponding to full use of the sorbent. In mono-component systems, Zn(II) breakthrough (corresponding to 25 h of operation) occurs faster than Cd(II) (operating time: 40 h). This result agrees with the order of the Langmuir affinity coefficients found in batch experiments. The mass transfer zone (MTZ) is another parameter frequently used to examine the effective height of a sorption column. MTZ is the active part of the fixed bed where adsorption actually operates; Length unused bed (LUB) is the part of the column where adsorption does not take place. In our case, the LUB part is 16% in the Zn(II)-loaded column, and 32% in the Cd(II)-loaded column. The column uptake at saturation (q) was higher than the batch uptake (q_m). This may be due to the continuous formation of a large concentration gradient at the interface zone during column operation, which is the driving force for the adsorption process (Gupta et al., 2004). In case of batch adsorption isotherm studies such a concentration zone decreases with time (Gupta et al., 2004).

The values of t_b calculated with Thomas model were lower than those obtained from the curves (Table 6). Moreover, this model gave values of q_0 lower than those obtained from experimental data. All these facts confirm that the Thomas model underestimates the performance of the process at the beginning of the operation, which is in accordance with reported results (Calero et al., 2009). The Yoon and Nelson model was used for determining τ, (i.e., the time required to adsorb 50% of the initial concentration): which resulting 76 h and 71 h for Zn(II) and Cd(II), respectively. The correlation coefficients found for the three models are in general acceptable; however, the Dose-Response model showed the best fitting of the experimental data in all the measured range, as shown in Fig. 5.

The behavior of Ca(II) and pH was also evaluated during column operation. As shown in Fig. 5, the release of Ca(II) significantly increased before the t_b for each metal, remaining constant as the column began to saturate. The calcium present on the surface of the algal cell wall due the pretreatment applied was displaced by the heavy metal during the biosorption process. Its release varied depending with the heavy metal involved in the process: this confirms that ion exchange mechanism contributes to the biosorption of Zn(II) and Cd(II) on *U. pinnatifida*. The initial solution pH was regulated at 4.0 and 3.0 for Zn(II) and Cd(II) individual solutions. However, the effluent pH was between 6.0 and 7.0 at the beginning of column operation, and it decreased during heavy metal uptake till it reached the original solution pH at the end of the process. The same behavior for the pH was reported for Cr(III) adsorption by stones olives (Calero et al., 2009). The pH changes during the service time of the column could be attributed to proton uptake by the biosorbent. Insofar as the column was saturated, the adsorption capacity decreased and the pH reached the initial value.

The breakthrough curves of bi-component solutions were also obtained to study the competitive effect between metals and to evaluate the biosorbent selectivity for one metal in presence of the other in continuous system (Kleinübing et al., 2011) (Fig. 6). The t_b of Cd(II) was greater than Zn(II) and the Zn(II) curve reached saturation while Cd(II) did not reach it. Thomas, Yoon Nelson and Dose Response models were employed to fit the experimental data from bi-component solutions using fixed bed column. The parameters obtained are reported in Table 6. As Cd(II) did not reach saturation, Yoon Nelson model could not be applied in this case. In summary, t_b, t_e and q calculated with the models mentioned above as well as with the experimental data demonstrated the preference of *U. pinnatifida* for Cd(II) in the presence of Zn(II). Ca(II) and outlet pH during the bi-component column operation followed similar trends than those observed in mono-component columns demonstrated that ion exchange mechanisms is operating during the process.

The loaded-biomass recovered from mono- and bi-component columns were used in the desorption columns using 0.1 M HNO_3 as eluent. Fig. 7 shows the profiles of Zn(II) and Cd(II) release during the desorption column operation. The maximum desorption capacity was obtained in less than one hour. In bi-component desorption column the maximum desorption for Zn(II) was reached before Cd(II), reflecting once more the higher affinity of the biosorbent for Cd(II). The front of desorption curves for both metals are not very different, so the separate recovery of each metal could not be possible under the experimental conditions applied in this work. However, adjusting different experimental conditions like flow rate, columns height, etc. could increase the differences between the desorption curves allowing a selective recovery of each metals. The desorption of 64% of Zn(II) and about 83% of Cd(II) was achieved in mono-component desorption columns; while, when both metals were simultaneously present, 54% of Zn(II) and 70% of Cd(II) were recovered from metal-loaded biosorbent.

3.7. SEM-EDX, FT-IR analysis

The SEM-EDX analysis revealed that Zn(II) and Cd(II) were not uniformly distributed onto the surface of biosorbent (mono-component experiments). White aggregates were detected in the SEM micrographs (Fig. 8A and B): the EDX spectra of those spot gave a high signal corresponding to zinc or cadmium elements. However, in the case of loaded biomass from bi-component assays, it was not possible to detect those aggregates: the distribution of the two metals was homogeneous on biosorbent surface (Fig. 8C).

The FT-IR spectrum allows obtaining information about the functional groups involved in the uptake of heavy metals. Carboxylic groups are the main chemical groups that contribute in the adsorption on different biological materials (Yalçin et al., 2009).

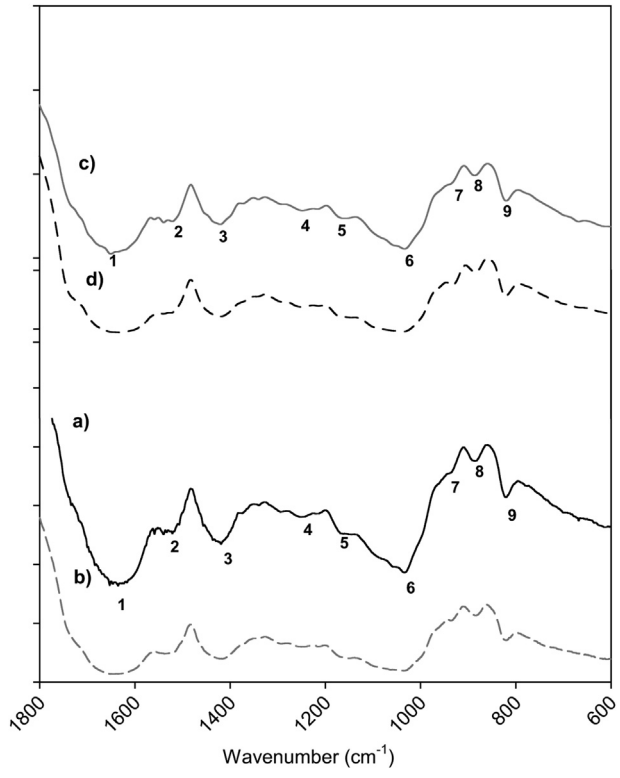

Fig. 9. FT-IR spectra of calcium-treated *U. pinnatifida* before and after Zn(II) and Cd(II) biosorption. a) and c) Control *U. pinnatifida* at pH 4 and 3, respectively; b) and d) *U. pinnatifida* loaded with Zn(II) (pH 4) and Cd(II) (pH 3), respectively. 1 to 9: peaks corresponding to functional groups on algal surface (Table 7).

Table 7
Main chemical groups in the FT-IR spectra involved in Zn(II) and Cd(II) biosorption using calcium-treated *U. pinnatifida* as biosorbent.

Functional groups	Up control pH = 4	Up loaded with Zn(II) pH = 4	Up control pH = 3	Up loaded with Cd(II) pH = 3
C═O asymmetric stretching of carboxyl	1637(1)	1642(1)	1641(1)	1647(1)
N–H deformation vibration of amida I groups	1520(2)	1537(2)	1515(2)	1520(2)
C═O symmetric stretching of carboxyl	1424(3)	1419(3)	1429(3)	1423(3)
COO vibration	1251(4)	1251(4)	1251(4)	1246(4)
C–O–C; C–O–P vibration	1039(6)	1033(6)	1032(6)	1027(6)
S═O; S–O; S–C symmetric and asymmetric stretching of sulfonate	1170(5)	1165(5)	1164(5)	1150(5)
	936(7)	931(7)	936(7)	930(7)
	880(8)	880(8)	890(8)	885(8)
	819(9)	819(9)	824(9)	819(9)

References: numbers (1) to (9) correspond to the peaks in FT-IR curves (Fig. 9).

Other chemical groups, containing S and N could also contribute to heavy metal uptake. Fig. 9 shows the FT-IR spectra corresponding to Zn(II) and Cd(II) loaded *U. pinnatifida*. The peak at 1647 cm^{-1} to 1637 cm^{-1} can be attributed to C═O stretching vibration of carboxylate groups or to its combined effect with N–H deformation vibration of amide I groups (Table 7). The asymmetric carboxyl stretching band shifted from 1642 cm^{-1} to 1637 cm^{-1} and from 1647 cm^{-1} to 1641 cm^{-1} after Zn(II) and Cd(II) binding, respectively. The distance between this band and the symmetric stretching of the same groups (at 1419 cm^{-1} and 1423 cm^{-1}) decreased to lower wave numbers after biosorption, indicating that chelating complexes were formed (Mata et al., 2008). The peaks at 1251 cm^{-1} and 1033 cm^{-1} are due to the C–O stretching vibration of ketones, aldehydes and lactones or carboxyl groups (Tan et al., 2011). Some shifts in wave numbers from 1251 cm^{-1} to 1246 cm^{-1} and 1039 cm^{-1} to 1033 cm^{-1}, were noticed in the spectra (Table 7), suggesting that COO vibration and C–O–C, C–O–P groups, respectively could contribute to biosorption process. Other functional groups, besides carboxyl groups, can participate to a lesser extent in biosorption; such as sulfyhydrils and sulfonates groups (Mata et al., 2008). Sulfonates were also active sites as shifts in the peaks corresponding to S═O stretching and S–O stretching were detected during Zn(II) and Cd(II) adsorption by *U. pinnatifida* (Fig. 9: peaks 5, 7, 8 and 9).

4. Conclusion

Considering that *U. pinnatifida* is an invasive alga responsible for changes in the biodiversity of Bahía de Camarones and Golfo Nuevo (Patagonia-Argentina) its recovery and use as biosorbent for wastewater loaded with heavy metals could represent an alternative to control its population growth. Data presented in this paper confirmed that calcium-treated *U. pinnatifida* is a suitable adsorbent for Zn(II) and Cd(II) pollutants. Experimental equilibrium data of metal adsorption in mono-component system have been well described by the Langmuir model and the affinity coefficient indicated that *U. pinnatifida* had preference for Cd(II) over Zn(II). In bi-component system, different mathematical models applied indicated the competition between metal ions: while some of the Cd(II) and Zn(II) ions are taken up with mutual competition, some active site may be specific to individual metals. A higher affinity for Cd(II) than Zn(II) was observed in bi components systems both in batch and columns experiments. The main mechanism responsible for Zn(II) and Cd(II) biosorption was ion exchange between calcium ions initial bound to the biomass and the heavy metals ions in solution. Apart from carboxylic groups, which can be considered the main chemical group contributing to Zn(II) and Cd(II) adsorption, other chemical groups, containing S and N also contribute to heavy metal uptake by Ca-treated *U. pinnatifida* biomass as determined by FT-IR analysis. The presence of sulfonate groups onto the cell wall of *U. pinnatifida* biomass could be one reason for the higher affinity for Cd(II) over Zn(II) as Cd(II) is a soft Lewis acid that forms strong bonds with ligands such as S or P. These active sites were not homogeneous distributed onto the cell wall as shown by the SEM-EDX analysis. Considering the different affinity of the biosorbent for both heavy metals, a selective recovery could be achieve adjusting the column design parameters (height, flow rate, etc).

The understanding of adsorption mechanisms of metals from mono and bi component batch and dynamic systems is necessary for development of appropriate management strategies for wastewater treatment.

Acknowledgments

Dr. Edgardo Donati and Dr. Marisa Viera are research members of CONICET. This research was supported by ANPCyT (PICT 339), CONICET (PIP 0368) and by the European Commission through the project BIOPROAM (II-0548-FC-FA).

Appendix A. Supplementary material

Supplementary data related to this article can be found online at http://dx.doi.org/10.1016/j.jenvman.2013.07.011.

References

Ahmady-Asbchin, S., Andrés, Y., Gérente, C., Le Cloirec, P., 2008. Biosorption of Cu(II) from aqueous solution by *Fucus serratus*: surface characterization and sorption mechanisms. Bioresour. Technol. 99, 6150–6155.
Ahmaruzzaman, M., 2011. Industrial wastes as low-cost potential adsorbents for the treatment of wastewater laden with heavy metals. Adv. Colloid Interface Sci. 166 (1–2), 36–59.
Areco, M.M., dos Santos Afonso, M., 2010. Copper, zinc, cadmium and lead biosorption by *Gymnogongrus torulosus*. Thermodynamics and kinetics studies. Colloids Surf. B. 81 (2), 620–628.
Arvizu-Higuera, D.L., Hernández-Carmona, G., Rodríguez-Montesinos, Y.E., 1995. Batch and continuous flow systems during the acid pre-extraction stage in the alginate extraction process. Ciencias Marinas. 1, 25–37.
Boschi, C., Maldonado, H., Ly, M., Guibal, E., 2011. Cd(II) biosorption using *Lessonia* kelps. J. Colloid Interf. Sci. 357 (2), 487–496.
Bulgariu, D., Bulgariu, L., 2011. Equilibrium and kinetics studies of heavy metal ions biosorption on green algae waste biomass. Bioresour. Technol. 103, 489–493.
Calero, M., Hernáinz, F., Blázquez, G., Tenorio, G., Martín-Lara, M., 2009. Study of Cr(III) biosorption in a fixed-bed column. J. Hazard. Mater. 171, 886–893.
Fagundes-Klen, M.R., Ferri, P., Martins, T.D., Tavares, C.R.G., Silva, E.A., 2007. Equilibrium study of binary mixture of cadmium-zinc ions biosorption by *Sargassum filipendula* species using adsorption isotherms models and neural network. Biochem. Eng. J. 34 (2), 136–146.
Gupta, V.K., Gupta, M., Sharma, S., 2001. Process development for the removal of lead and chromium from aqueous solutions using red mud-an aluminum industry waste. Water Res. 35 (5), 1125–1134.
Gupta, V.K., Mittal, A., Krishnan, L., Gajbe, V., 2004. Adsorption kinetics and column operations for the removal and recovery of malachite green from wastewater using bottom ash. Sep. Purif. Technol. 40 (1), 87–96.
Hawari, A.H., Mulligan, C.N., 2006. Heavy metals uptake mechanisms in a fixed-bed column by calcium-treated anaerobic biomass. Process. Biochem. 41 (1), 187–198.

Ho, Y., 2006. Second order kinetic model for sorption of cadmium onto tree fern: a comparison of linear and non – linear methods. Water Res. 40, 119–125.
Kleinübing, S.J., Silva, E.A., da Silva, M.G.C., Guibal, E., 2011. Equilibrium of Cu(II) and Ni(II) biosorption by marine alga *Sargassum filipendula* in a dynamic system: competitiveness and selectivity. Bioresour. Technol. 102, 4610–4617.
Kurniawan, T.A., Chan, G.Y.S., Lo, W.-H., Babel, S., 2006. Comparison of low-cost adsorbents for treating wastewaters laden with heavy metals. Sci. Total Environ. 366 (2–3), 409–426.
Lee, S.-W., Park, H.-J., Lee, S.-H., Lee, M.-G., 2008. Comparison of adsorption characteristics according to polarity difference of acetone vapor and toluene vapor on silica–alumina fixed-bed reactor. J. Ind. Eng. Chem. 14 (1), 10–17.
Lodeiro, P., Barriada, J.L., Herrero, R., Sastre de Vicente, M.E., 2006. The marine macroalga *Cystoseira baccata* as biosorbent for cadmium(II) and lead(II) removal: kinetic and equilibrium studies. Environ. Pollut. 142 (2), 264–273.
Luna, A.S., Costa, A.L.H., da Costa, A.C.A., Henriques, C.A., 2010. Competitive biosorption of cadmium (II) and zinc (II) ions from binary systems by *Sargassum filipendula*. Bioresour. Technol. 101, 5104–5111.
Martins, R.J.E., Pardo, R., Boaventura, R.A.R., 2004. Cadmium(II) and zinc(II) adsorption by the aquatic moss *Fontinalis antipyretica*: effect of temperature, pH and water hardness. Water Res. 38, 693–699.
Mata, Y.N., Blázquez, M.L., Ballester, A., González, F., Muñoz, J.A., 2008. Characterization of the biosorption of cadmium, lead and copper with the brown alga *Fucus vesiculosus*. J. Hazard. Mater. 158, 316–323.
Matheickal, J.T., Qiming, Y., 1999. Biosorption of lead(II) and copper(II) from aqueous solutions by pre-treated biomass of *Australian marine* algae. Bioresour. Technol. 69, 3094–3099.
Montazer-Rahmatia, M.M., Rabbania, R., Abdolalia, A., Keshtkarb, A.R., 2011. Kinetics and equilibrium studies on biosorption of cadmium, lead, and nickel ions from aqueous solutions by intact and chemically modified brown algae. J. Hazard. Mater. 185, 401–407.
Oliveira, R.C., Jouannin, C., Guibal, E., Garcia Jr., O., 2011. Samarium(III) and praseodymium(III) biosorption on *Sargassum* sp.: batch study. Process. Biochem. 46, 736–744.
Peric, J., Trgo, M., Vukojevic Medvidovic, N., 2004. Removal of zinc, copper and lead by natural zeolite-a comparison of adsorption isotherms. Water Res. 38, 1893–1899.
Plaza, J., Viera, M., Donati, E., Guibal, E., 2011. Biosorption of mercury by *Macrocystis pyrifera* and *Undaria pinnatifida*: influence of zinc, cadmium and nickel. J. Environ. Sci. 23 (11), 1778–1786.
Plaza, J., Bernardelli, C., Viera, M., Donati, E., Guibal, E., 2012. Zinc and cadmium biosorption by untreated and Calcium-treated *Macrocystis pyrifera* in a batch system. Bioresour. Technol. 116, 195–203.
Plaza Cazón, J., Benítez, L., Donati, E., Viera, M., 2012. Biosorption of chromium (III) by two brown algae *Macrocystis pyrifera* and *Undaria pinnatifida*: equilibrium and kinetic study. Eng. Life Sci. 12 (1), 95–103.
Remenárová, L., Pipíška, M., Horník, M., Rozložník, M., Agustín, J., Lesny, J., 2012. Biosorption of cadmium and zinc by activated sludge from single and binary solutions: mechanism, equilibrium and experimental design study. J. Taiwan Inst. Chem. E 43 (3), 433–443.
Rahelivao, P.M., Andriamanantoanina, H., Heyraud, A., Rinaudo, M., 2013. Short communication: structure and properties of three alginates from Madagascan seacoast algae. Food Hydrocoll. 32, 143–146.
Sari, A., Tuzen, M., Uluözlü, O.D., Soylak, M., 2007. Biosorption of Pb(II) and Ni(II) from aqueous solution by lichen (*Cladonia furcata*) biomass. Biochem. Eng. J. 37, 151–158.
Sheng, P.X., Ting, Y.P., Chen, P., Hong, L., 2004. Sorption of lead, cooper, cadmium, zinc and nickel by marine biomass: characterization of biosorptive capacity and investigation of mechanisms. J. Colloid Interf. Sci. 275, 131–141.
Svecova, L., Spanelova, M., Kubal, M., Guibal, E., 2006. Cadmium, lead and mercury biosorption on waste fungal biomass issued from fermentation industry. I. Equilibrium studies. Sep. Purif. Technol. 52, 142–153.
Tan, C., Li, M., Lin, Y., Lu, X., Chen, Z., 2011. Biosorption of basic orange from aqueous solution onto dried *A. filiculoides* biomass: equilibrium, kinetic and FTIR studies. Desalination 266, 56–62.
Velazquez-Jimenez, L.H., Pavlick, A., Rangel-Mendez, J.R., 2013. Chemical characterization of raw and treated agave bagasse and its potential as adsorbent of metal cations from water. Ind. Crop Prod. 43, 200–206.
Volesky, B., 2003. Sorption and Biosorption. B. V. Sorbex, Inc., Montreal-St. Lambert, Quebec, Canada.
Wilson, D., del Valle, M., Alegret, S., Valderrama, C., Florido, A., 2012. Potentiometric electronic tongue-flow injection analysis system for the monitoring of heavy metal biosorption processes. Talanta 93, 285–292.
Yalçin, E., Çavuşo, K., Kinalio, K., 2009. Biosorption of Cu^{2+} and Zn^{2+} by raw and autoclave *Rocella phycopsis*. J. Environ. Sci. 22, 367–373.
Zhang, Y., Banks, C., 2006. A comparison of the properties of polyurethane immobilised Sphagnum moss, seaweed, sunflower waste and maize for the biosorption of Cu, Pb, Zn and Ni in continuous flow packed columns. Water Res. 40, 788–798.